Light-Front Holography and Novel Effects in QCD

Stanley J. Brodsky* and Guy F. de Téramond†

*SLAC National Accelerator Laboratory, Stanford University, Stanford, CA 94309, USA
†Universidad de Costa Rica, San José, Costa Rica

Abstract.
   The correspondence between theories in anti-de Sitter space and conformal field theories in physical space-time leads to an analytic, semiclassical model for strongly-coupled QCD. Light-front holography allows hadronic amplitudes in the AdS fifth dimension to be mapped to frame-independent light-front wavefunctions of hadrons in physical space-time, thus providing a relativistic description of hadrons at the amplitude level. We identify the AdS coordinate z with an invariant light-front coordinate ζ which separates the dynamics of quark and gluon binding from the kinematics of constituent spin and internal orbital angular momentum. The result is a single-variable light-front Schrödinger equation for QCD which determines the eigenspectrum and the light-front wavefunctions of hadrons for general spin and orbital angular momentum. The mapping of electromagnetic and gravitational form factors in AdS space to their corresponding expressions in light-front theory confirms this correspondence. Some novel features of QCD are discussed, including the consequences of confinement for quark and gluon condensates and the behavior of the QCD coupling in the infrared. The distinction between static structure functions such as the probability distributions computed from the square of the light-front wavefunctions versus dynamical structure functions which include the effects of rescattering is emphasized. A new method for computing the hadronization of quark and gluon jets at the amplitude level, an event amplitude generator, is outlined.

INTRODUCTION

One of the most challenging problems in strong interaction dynamics is to understand the interactions and composition of hadrons in terms of the fundamental quark and gluon degrees of freedom of the QCD Lagrangian. Because of the strong-coupling of QCD in the infrared domain, it has been difficult to find analytic solutions for the wavefunctions of hadrons or to make precise predictions for hadronic properties outside of the perturbative regime. Thus an important theoretical goal is to find an initial approximation to bound-state problems in QCD which is analytically tractable and which can be systematically improved. The AdS/CFT correspondence [1] between string states in anti–de Sitter (AdS) space and conformal field theories in physical space-time, modified for color confinement, has led to a semiclassical model for strongly-coupled QCD which provides analytical insights into its inherently non-perturbative nature, including hadronic spectra, decay constants, and wavefunctions.

   As we have recently shown [2, 3], there is a remarkable correspondence between the AdS description of hadrons and the Hamiltonian formulation of QCD in physical

space-time quantized on the light front. A key feature is "light-front holography" which allows one to precisely map the AdS_5 solutions $\Phi(z)$ for hadron amplitudes in the fifth dimensional variable z to light-front wavefunctions $\psi_{n/H}$ of hadrons in the light-front coordinate ζ in physical space-time [2, 3], thus providing a relativistic description of hadrons in QCD at the amplitude level. For two particles $\zeta^2 = \mathbf{b}_\perp^2 x(1-x)$ which is conjugate to the invariant mass squared $\mathcal{M}^2$ of the pair and also their light-front kinetic energy $\mathbf{k}_\perp^2/x(1-x)$. One can derive this connection by showing that one obtains the identical holographic mapping using the matrix elements of the electromagnetic current and the energy-momentum tensor [4]; this gives an important consistency test and verification of holographic mapping from AdS to physical observables defined on the light front. The mathematical consistency of light-front holography for both the electromagnetic and gravitational [4] hadronic transition matrix elements demonstrates that the mapping between the AdS holographic variable z and the transverse light-front variable ζ, which is a function of the multi-dimensional coordinates of the partons in a given light-front Fock state $x_i, \mathbf{b}_{\perp i}$ at fixed light-front time τ, is a general principle.

Our analysis follows from recent developments in light-front QCD [2, 3, 4, 5, 6, 7] which have been inspired by the AdS/CFT correspondence [1] between string states in anti-de Sitter (AdS) space and conformal field theories (CFT) in physical space-time. Conformal symmetry is broken in physical QCD by quantum effects and quark masses. The application of AdS space and conformal methods to QCD can be motivated from the empirical evidence [8] and theoretical arguments [9] that the QCD coupling $\alpha_s(Q^2)$ has an infrared fixed point at small Q^2. In particular, a new extraction of the effective strong coupling constant $\alpha_s^{g_1}(Q^2)$ from CLAS spin structure function data in an extended Q^2 region using the Bjorken sum rule $\Gamma_1^{p-n}(Q^2)$ [8], indicates the lack of Q^2 dependence of α_s in the low Q^2 limit. One can understand this physically: in a confining theory where gluons have an effective mass [10] or the quarks and gluons have maximal wavelength [9], all vacuum polarization corrections to the gluon self-energy decouple at long wavelength. Thus an infrared fixed point appears to be a natural consequence of confinement. Furthermore, if one considers a semiclassical approximation to QCD with massless quarks and without particle creation or absorption, then the resulting β function is zero, the coupling is constant, and the approximate theory is scale and conformal invariant [11]. One can then use conformal symmetry as a *template*, systematically correcting for its nonzero β function as well as higher-twist effects [12]. In particular, we can use the mapping of the group of Poincare and conformal generators $SO(4,2)$ to the isometries of AdS_5 space. The fact that gluons have maximum wavelengths and hence minimum momenta provides an explanation for why multiple emission of soft gluons with large couplings does not spoil the Appelquist-Politzer argument for the narrowness of J/ψ and Υ; the explanation is that such emission is kinematically forbidden [9].

In this lecture we review some of the features of the "hard-wall" [13] and "soft-wall" [14] AdS/QCD models [15, 16] which provide an initial approximation to QCD. In our approach the holographic mapping is carried out in the strongly coupled regime where QCD is almost conformal, but in contrast with the AdS/QCD framework described in [14, 15, 16] quark and gluon degrees of freedom are explicitly introduced in the gauge/gravity correspondence. Consequently, the identification of orbital angular momentum of the constituents becomes a key element in the description of the internal

structure of hadrons using holographic principles. To this end, we also will discuss a procedure based on the light-front Hamiltonian of QCD [17] which in principle allows the model to be systematically improved.

Some of the important features of light-front AdS/QCD include:

(1) Effective frame-independent single-particle Schödinger and Dirac equations for meson and baryon wave equations in both z and ζ. For example, the meson eigenvalue equation is

$$\left[-\frac{d^2}{dz^2} - \frac{1-4L^2}{4z^2} + U(z)\right]\phi(z) = \mathcal{M}^2\phi(z).$$

where the soft-wall potential has the form of a harmonic oscillator $U(z) = \kappa^4 z^2 + 2\kappa^2(L+S-1)$.

(2) The mass spectra formula for mesons at zero quark mass in the soft-wall model is

$$\mathcal{M}^2 = 4\kappa^2(n+L+S/2),$$

which agrees with conventional Regge phenomenology. As in the Nambu string model based on a rotating flux tube, the Regge slope is the same for both the principal quantum number n and the orbital angular momentum L. The AdS/QCD correspondence thus builds in a remarkable connection between the string mass μ in the string theory underlying an effective gravity theory in the fifth dimension with the orbital angular momentum of hadrons in physical space-time.

(3) The pion is massless at zero quark mass in agreement with general arguments based on chiral symmetry.

(4) The predicted form factors for the pion and nucleons agree well with experiment. The nucleon LFWFs have both S and P wave-components allowing one to compute both the Dirac and Pauli form factors. In general the AdS/QCD form factors fall off in momentum transfer squared q^2 with a leading power predicted by the dimensional counting rules and the leading twist of the hadron's dominant interpolating operator at short distances. The short-distance behavior of a hadronic state is characterized by its twist (dimension minus spin) $\tau = \Delta - \sigma$, where σ is the sum over the constituent's spin $\sigma = \sum_{i=1}^{n} \sigma_i$. Twist is also equal to the number of partons $\tau = n$ if $L = 0$. Under conformal transformations the interpolating operators transform according to their twist, and consequently the AdS isometries map the twist scaling dimensions into the AdS modes [6]. Light-front holography thus provide a simple semiclassical approximation to QCD which has both constituent counting rule behavior [18, 19] at short distances and confinement at large distances [5, 13].

(5) The timelike form factors of hadrons exhibit poles in the $J^{PC} = 1^{--}$ vector meson channels, an analytic feature which arises from the dressed electromagnetic current in AdS/QCD [3, 20].

(6) The form of the nonperturbative pion distribution amplitude $\phi_\pi(x)$ obtained from integrating the $q\bar{q}$ valence LFWF $\psi(x, \mathbf{k}_\perp)$ over $\mathbf{k}_\perp$, has a quite different x-behavior than the asymptotic distribution amplitude predicted from the ERBL PQCD evolution [21, 22] of the pion distribution amplitude. The AdS prediction $\phi_\pi(x) = \sqrt{3}f_\pi\sqrt{x(1-x)}$ has a broader distribution than expected from solving the ERBL evolution equation in perturbative QCD. This observation appears to be consistent with the results of the

Fermilab diffractive dijet experiment [23], the moments obtained from lattice QCD [5] and pion form factor data [24].

LIGHT-FRONT HOLOGRAPHY

One of the most important theoretical tools in atomic physics is the Schrödinger equation, which describes the quantum-mechanical structure of atomic systems at the amplitude level. Light-front wavefunctions (LFWFs) play a similar role in quantum chromodynamics, providing a fundamental description of the structure and internal dynamics of hadrons in terms of their constituent quarks and gluons. The light-front wavefunctions of bound states in QCD are relativistic generalizations of the Schrödinger wavefunctions of atomic physics, but they are determined at fixed light-cone time $\tau = t + z/c$ – the "front form" introduced by Dirac [25] – rather than at fixed ordinary time t. A remarkable feature of LFWFs is the fact that they are frame independent; i.e., the form of the LFWF is independent of the hadron's total momentum $P^+ = P^0 + P^3$ and $\vec{P}_\perp$.

When a flash from a camera illuminates a scene, each object is illuminated along the light-front of the flash; i.e., at a given τ. Similarly, when a sample is illuminated by an x-ray source such as the Linac Coherent Light Source, each element of the target is struck at a given τ. In contrast, setting the initial condition using conventional instant time t requires simultaneous scattering of photons on each constituent. Thus it is natural to set boundary conditions at fixed τ and then evolve the system using the light-front Hamiltonian $P^- = P^0 - P^3 = id/d\tau$. The invariant Hamiltonian $H_{LF} = P^+P^- - P_\perp^2$ then has eigenvalues $\mathcal{M}^2$ where $\mathcal{M}$ is the physical mass. Its eigenfunctions are the light-front eigenstates whose Fock state projections define the light-front wavefunctions.

Light-front quantization is the ideal framework to describe the structure of hadrons in terms of their quark and gluon degrees of freedom. The simple structure of the light-front vacuum allows an unambiguous definition of the partonic content of a hadron. Given the LFWFs, one can compute observables such as hadronic form factors and structure functions, as well as the generalized parton distributions and distribution amplitudes which underly hard exclusive reactions. The constituent spin and orbital angular momentum properties of the hadrons are also encoded in the LFWFs.

A key step in the analysis of an atomic system such as positronium is the introduction of the spherical coordinates r, θ, ϕ which separates the dynamics of Coulomb binding from the kinematical effects of the quantized orbital angular momentum L. The essential dynamics of the atom is specified by the radial Schrödinger equation whose eigensolutions $\psi_{n,L}(r)$ determine the bound-state wavefunction and eigenspectrum. In this paper, we show that there is an analogous invariant light-front coordinate ζ which allows one to separate the essential dynamics of quark and gluon binding from the kinematical physics of constituent spin and internal orbital angular momentum. The result is a single-variable light-front Schrödinger equation for QCD which determines the eigenspectrum and the light-front wavefunctions of hadrons for general spin and orbital angular momentum.

Light-Front Holography can be derived by observing the correspondence between matrix elements obtained in AdS/CFT with the corresponding formula using the LF representation [2] . The light-front electromagnetic form factor in impact space [2, 3, 26] can be written as a sum of overlap of light-front wave functions of the $j = 1, 2, \cdots, n - 1$

spectator constituents:

$$F(q^2) = \sum_n \prod_{j=1}^{n-1} \int dx_j d^2\mathbf{b}_{\perp j} \sum_q e_q \exp\left(i\mathbf{q}_\perp \cdot \sum_{j=1}^{n-1} x_j \mathbf{b}_{\perp j}\right) \left|\tilde{\psi}_n(x_j, \mathbf{b}_{\perp j})\right|^2. \tag{1}$$

The formula is exact if the sum is over all Fock states n. For definiteness we shall consider a two-quark π^+ valence Fock state $|u\bar{d}\rangle$ with charges $e_u = \frac{2}{3}$ and $e_{\bar{d}} = \frac{1}{3}$. For $n = 2$, there are two terms which contribute to the q-sum in (1). Exchanging $x \leftrightarrow 1-x$ in the second integral we find ($e_u + e_{\bar{d}} = 1$)

$$\begin{aligned} F_{\pi^+}(q^2) &= \int_0^1 dx \int d^2\mathbf{b}_\perp e^{i\mathbf{q}_\perp \cdot \mathbf{b}_\perp (1-x)} \left|\tilde{\psi}_{u\bar{d}/\pi}(x, \mathbf{b}_\perp)\right|^2 \\ &= 2\pi \int_0^1 \frac{dx}{x(1-x)} \int \zeta d\zeta J_0\left(\zeta q \sqrt{\frac{1-x}{x}}\right) \left|\tilde{\psi}_{u\bar{d}/\pi}(x, \zeta)\right|^2, \end{aligned} \tag{2}$$

where $\zeta^2 = x(1-x)\mathbf{b}_\perp^2$ and $F_\pi^+(q=0) = 1$. Notice that by performing an identical calculation for the π^0 meson the result is $F_{\pi^0}(q^2) = 0$ for any value of q, as expected from C-charge conjugation invariance.

We now compare this result with the electromagnetic form-factor in AdS space [27]:

$$F(Q^2) = R^3 \int \frac{dz}{z^3} J(Q^2, z)|\Phi(z)|^2, \tag{3}$$

where $J(Q^2, z) = zQK_1(zQ)$. Using the integral representation of $J(Q^2, z)$

$$J(Q^2, z) = \int_0^1 dx J_0\left(\zeta Q \sqrt{\frac{1-x}{x}}\right), \tag{4}$$

we can write the AdS electromagnetic form-factor as

$$F(Q^2) = R^3 \int_0^1 dx \int \frac{dz}{z^3} J_0\left(zQ \sqrt{\frac{1-x}{x}}\right) |\Phi(z)|^2. \tag{5}$$

Comparing with the light-front QCD form factor (2) for arbitrary values of Q

$$|\tilde{\psi}(x, \zeta)|^2 = \frac{R^3}{2\pi} x(1-x) \frac{|\Phi(\zeta)|^2}{\zeta^4}, \tag{6}$$

where we identify the transverse light-front variable ζ, $0 \le \zeta \le \Lambda_{\text{QCD}}$, with the holographic variable z.

Matrix elements of the energy-momentum tensor $\Theta^{\mu\nu}$ which define the gravitational form factors play an important role in hadron physics. Since one can define $\Theta^{\mu\nu}$ for each parton, one can identify the momentum fraction and contribution to the orbital angular momentum of each quark flavor and gluon of a hadron. For example, the spin-flip form factor $B(q^2)$, which is the analog of the Pauli form factor $F_2(Q^2)$ of a nucleon, provides

a measure of the orbital angular momentum carried by each quark and gluon constituent of a hadron at $q^2 = 0$. Similarly, the spin-conserving form factor $A(q^2)$, the analog of the Dirac form factor $F_1(q^2)$, allows one to measure the momentum fractions carried by each constituent. This is the underlying physics of Ji's sum rule [28]: $\langle J^z \rangle = \frac{1}{2}[A(0) + B(0)]$, which has prompted much of the current interest in the generalized parton distributions (GPDs) measured in deeply virtual Compton scattering. Measurements of the GDP's are of particular relevance for determining the distribution of partons in the transverse impact plane, and thus could be confronted with AdS/QCD predictions which follow from the mapping of AdS modes to the transverse impact representation [2]. An important constraint is $B(0) = \sum_i B_i(0) = 0$; i.e. the anomalous gravitomagnetic moment of a hadron vanishes when summed over all the constituents i. This was originally derived from the equivalence principle of gravity [29]. The explicit verification of these relations, Fock state by Fock state, can be obtained in the light-front quantization of QCD in light-cone gauge [30]. Physically $B(0) = 0$ corresponds to the fact that the sum of the n orbital angular momenta L in an n-parton Fock state must vanish since there are only $n - 1$ independent orbital angular momenta.

The light-front expression for the helicity-conserving gravitational form factor in impact space is [4]

$$A(q^2) = \sum_n \prod_{j=1}^{n-1} \int dx_j d^2 \mathbf{b}_{\perp j} \sum_f x_f \exp\left(i\mathbf{q}_\perp \cdot \sum_{j=1}^{n-1} x_j \mathbf{b}_{\perp j}\right) \left|\tilde{\psi}_n(x_j, \mathbf{b}_{\perp j})\right|^2, \qquad (7)$$

which includes the contribution of each struck parton with longitudinal momentum x_f and corresponds to a change of transverse momentum $x_j \mathbf{q}$ for each of the $j = 1, 2, \cdots, n - 1$ spectators. For $n = 2$, there are two terms which contribute to the f-sum in (7). Exchanging $x \leftrightarrow 1 - x$ in the second integral we find

$$
\begin{aligned}
A_\pi(q^2) &= 2\int_0^1 x\,dx \int d^2 \mathbf{b}_\perp\, e^{i\mathbf{q}_\perp \cdot \mathbf{b}_\perp (1-x)} \left|\tilde{\psi}(x, \mathbf{b}_\perp)\right|^2 \\
&= 4\pi \int_0^1 \frac{dx}{(1-x)} \int \zeta\,d\zeta\, J_0\left(\zeta q \sqrt{\frac{1-x}{x}}\right) |\tilde{\psi}(x, \zeta)|^2, \qquad (8)
\end{aligned}
$$

where $\zeta^2 = x(1-x)\mathbf{b}_\perp^2$. We now consider the expression for the hadronic gravitational form factor in AdS space [31]

$$A_\pi(Q^2) = R^3 \int \frac{dz}{z^3} H(Q^2, z) |\Phi_\pi(z)|^2, \qquad (9)$$

where $H(Q^2, z) = \frac{1}{2}Q^2 z^2 K_2(zQ)$. The hadronic form factor is normalized at $Q = 0$, $A(0) = 1$. Using the integral representation of $H(Q^2, z)$

$$H(Q^2, z) = 2\int_0^1 x\,dx\, J_0\left(zQ\sqrt{\frac{1-x}{x}}\right), \qquad (10)$$

we can write the AdS gravitational form factor

$$A(Q^2) = 2R^3 \int_0^1 x\, dx \int \frac{dz}{z^3} J_0\left(zQ\sqrt{\frac{1-x}{x}}\right) |\Phi(z)|^2.$$

(11)

Comparing with the QCD gravitational form factor (8) we find an identical relation between the light-front wave function $\tilde{\psi}(x,\zeta)$ and the AdS wavefunction $\Phi(z)$ given in Eq. (6) which is obtained from the mapping of the pion electromagnetic transition amplitude.

LIGHT-FRONT QUANTIZATION OF QCD

One can express the hadron four-momentum generator $P = (P^+, P^-, \mathbf{P}_\perp)$, $P^\pm = P^0 \pm P^3$, in terms of the dynamical fields, the Dirac field ψ_+, $\psi_\pm = \Lambda_\pm \psi$, $\Lambda_\pm = \gamma^0 \gamma^\pm$, and the transverse field $\mathbf{A}_\perp$ in the $A^+ = 0$ gauge [32]

$$
\begin{aligned}
P^- &= \frac{1}{2}\int dx^- d^2\mathbf{x}_\perp\, \bar{\psi}_+ \gamma^+ \frac{m^2 + (i\nabla_\perp)^2}{i\partial^+} \psi_+ + \text{interactions}, \\
P^+ &= \int dx^- d^2\mathbf{x}_\perp\, \bar{\psi}_+ \gamma^+ i\partial^+ \psi_+, \\
\mathbf{P}_\perp &= \frac{1}{2}\int dx^- d^2\mathbf{x}_\perp\, \bar{\psi}_+ \gamma^+ i\nabla_\perp \psi_+,
\end{aligned}
$$

(12)

where the integrals are over the initial surface $x^+ = 0$, $x^\pm = x^0 \pm x^3$. The operator P^- generates LF time translations $[\psi_+(x), P^-] = i\frac{\partial}{\partial x^+}\psi_+(x)$, and the generators P^+ and $\mathbf{P}_\perp$ are kinematical. For simplicity we have omitted from (12) the contribution from the gluon field $\mathbf{A}_\perp$.

The Dirac field operator is expanded as

$$\psi_+(x^-, \mathbf{x}_\perp)_\alpha = \sum_\lambda \int_{q^+>0} \frac{dq^+}{\sqrt{2q^+}} \frac{d^2\mathbf{q}_\perp}{(2\pi)^3} \left[b_\lambda(q) u_\alpha(q,\lambda) e^{-iq\cdot x} + d_\lambda(q)^\dagger v_\alpha(q,\lambda) e^{iq\cdot x} \right],$$

(13)

with u and v LF spinors [33]. Similar expansion follows for the gluon field $\mathbf{A}_\perp$. Using LF commutation relations $\{b(q), b^\dagger(q')\} = (2\pi)^3 \delta(q^+ - q'^+)\delta^{(2)}(\mathbf{q}_\perp - \mathbf{q}'_\perp)$, we find

$$P^- = \sum_\lambda \int \frac{dq^+ d^2\mathbf{q}_\perp}{(2\pi)^3} \frac{m^2 + \mathbf{q}_\perp^2}{q^+} b_\lambda^\dagger(q) b_\lambda(q) + \text{interactions},$$

and we recover the LF dispersion relation $q^- = (\mathbf{q}_\perp^2 + m^2)/q^+$, which follows from the on shell relation $q^2 = m^2$. The LF time evolution operator P^- is conveniently written as a term which represents the sum of the kinetic energy of all the partons plus a sum of all the interaction terms.

It is convenient to define a LF Lorentz invariant Hamiltonian $H_{LF} = P_\mu P^\mu = P^- P^+ - \mathbf{P}_\perp^2$ with eigenstates $|\psi_H(P^+, \mathbf{P}_\perp, S_z)\rangle$ and eigenmass $\mathcal{M}_H^2$, the mass spectrum of the

color-singlet states of QCD [32]

$$H_{LF}|\psi_H\rangle = \mathcal{M}_H^2|\psi_H\rangle. \tag{14}$$

A state $|\psi_H\rangle$ is an expansion in multi-particle Fock states $|n\rangle$ of the free LF Hamiltonian: $|\psi_H\rangle = \sum_n \psi_{n/H}|n\rangle$, where a one parton state is $|q\rangle = \sqrt{2q^+}\,b^\dagger(q)|0\rangle$. The Fock components $\psi_{n/H}(x_i, \mathbf{k}_{\perp i}, \lambda_i^z)$ are independent of P^+ and $\mathbf{P}_\perp$ and depend only on relative partonic coordinates: the momentum fraction $x_i = k_i^+/P^+$, the transverse momentum $\mathbf{k}_{\perp i}$ and spin component λ_i^z. Momentum conservation requires $\sum_{i=1}^n x_i = 1$ and $\sum_{i=1}^n \mathbf{k}_{\perp i} = 0$. The LFWFs $\psi_{n/H}$ provide a *frame-independent* representation of a hadron which relates its quark and gluon degrees of freedom to their asymptotic hadronic state.

We can compute $\mathcal{M}^2$ from the hadronic matrix element

$$\langle \psi_H(P')|H_{LF}|\psi_H(P)\rangle = \mathcal{M}_H^2\langle \psi_H(P')|\psi_H(P)\rangle, \tag{15}$$

expanding the initial and final hadronic states in terms of its Fock components. The computation is much simplified in the frame $P = \left(P^+, M^2/P^+, \vec{0}_\perp\right)$ where $H_{LF} = P^+P^-$. We find

$$\mathcal{M}_H^2 = \sum_n \int [dx_i]\,[d^2\mathbf{k}_{\perp i}] \sum_q \left(\frac{m_q^2 + \mathbf{k}_{\perp q}^2}{x_q}\right) \left|\psi_{n/H}(x_i, \mathbf{k}_{\perp i})\right|^2 + \text{interactions}, \tag{16}$$

plus similar terms for antiquarks and gluons ($m_g = 0$). The integrals in (16) are over the internal coordinates of the n constituents for each Fock state with phase space normalization

$$\sum_n \int [dx_i]\,[d^2\mathbf{k}_{\perp i}] \left|\psi_{n/H}(x_i, \mathbf{k}_{\perp i})\right|^2 = 1. \tag{17}$$

The LFWF $\psi_n(x_i, \mathbf{k}_{\perp i})$ can be expanded in terms of $n-1$ independent position coordinates $\mathbf{b}_{\perp j}$, $j = 1, 2, \ldots, n-1$, so that $\sum_{i=1}^n \mathbf{b}_{\perp i} = 0$. We can also express (16) in terms of the internal coordinates $\mathbf{b}_{\perp j}$ with $\mathbf{k}_\perp^2 \to -\nabla_{\mathbf{b}_\perp}^2$. The normalization is defined by

$$\sum_n \prod_{j=1}^{n-1} \int dx_j d^2\mathbf{b}_{\perp j}|\psi_{n/H}(x_j, \mathbf{b}_{\perp j})|^2 = 1. \tag{18}$$

To simplify the discussion we will consider a two-parton hadronic bound state. In the limit $m_q \to 0$

$$
\begin{aligned}
\mathcal{M}^2 &= \int_0^1 dx \int \frac{d^2\mathbf{k}_\perp}{16\pi^3} \frac{\mathbf{k}_\perp^2}{x(1-x)} |\psi(x, \mathbf{k}_\perp)|^2 + \text{interactions} \\
&= \int_0^1 \frac{dx}{x(1-x)} \int d^2\mathbf{b}_\perp\, \psi^*(x, \mathbf{b}_\perp)\left(-\nabla_{\mathbf{b}_\perp}^2\right)\psi(x, \mathbf{b}_\perp) + \text{interactions}.
\end{aligned} \tag{19}
$$

It is clear from (19) that the functional dependence for a given Fock state is given in terms of the invariant mass

$$\mathcal{M}_n^2 = \left(\sum_{a=1}^n k_a^\mu\right)^2 = \sum_a \frac{\mathbf{k}_{\perp a}^2}{x_a} \to \frac{\mathbf{k}_\perp^2}{x(1-x)}, \tag{20}$$

the measure of the off-mass shell energy $\mathcal{M}^2 - \mathcal{M}_n^2$. Similarly in impact space the relevant variable for a two-parton state is $\zeta^2 = x(1-x)\mathbf{b}_\perp^2$. Thus, to first approximation LF dynamics depend only on the boost invariant variable $\mathcal{M}_n$ or ζ, and hadronic properties are encoded in the hadronic mode $\phi(\zeta)$ from the relation

$$\psi(x, \zeta) = \frac{\phi(\zeta)}{\sqrt{2\pi\zeta}} f(x). \tag{21}$$

We choose the normalization of the LF mode $\phi(\zeta) = \langle \zeta | \phi \rangle$

$$\langle \phi | \phi \rangle = \int d\zeta \, |\langle \zeta | \phi \rangle|^2 = 1, \tag{22}$$

and thus the prefactor $f(x)$ is normalized according to $\int_0^1 \frac{dx}{x(1-x)} |f(x)|^2 = 1$. The mapping of transition matrix elements for arbitrary values of the momentum transfer [2, 4] gives $f(x) = \sqrt{x(1-x)}$.

We can write the Laplacian operator in (19) in circular cylindrical coordinates (ζ, φ) with $\zeta = \sqrt{x(1-x)}|\mathbf{b}_\perp|$: $\nabla^2 = \frac{1}{\zeta} \frac{d}{d\zeta}\left(\zeta \frac{d}{d\zeta}\right) + \frac{1}{\zeta^2} \frac{\partial^2}{\partial\varphi^2}$, and factor out the angular dependence of the modes in terms of the $SO(2)$ Casimir representation L^2 of orbital angular momentum in the transverse plane: $\phi(\zeta, \varphi) \sim e^{\pm iL\varphi} \phi(\zeta)$. Using (21) we find [17]

$$
\begin{aligned}
\mathcal{M}^2 &= \int d\zeta \, \phi^*(\zeta) \sqrt{\zeta} \left(-\frac{d^2}{d\zeta^2} - \frac{1}{\zeta}\frac{d}{d\zeta} + \frac{L^2}{\zeta^2} \right) \frac{\phi(\zeta)}{\sqrt{\zeta}} + \int d\zeta \, \phi^*(\zeta) U(\zeta) \phi(\zeta) \\
&= \int d\zeta \, \phi^*(\zeta) \left(-\frac{d^2}{d\zeta^2} - \frac{1 - 4L^2}{4\zeta^2} + U(\zeta) \right) \phi(\zeta),
\end{aligned}
$$

where all the complexity of the interaction terms in the QCD Lagrangian is summed up in the effective potential $U(\zeta)$. The light-front eigenvalue equation $H_{LF} |\phi\rangle = \mathcal{M}^2 |\phi\rangle$ is thus a light-front wave equation for ϕ

$$\left(-\frac{d^2}{d\zeta^2} - \frac{1 - 4L^2}{4\zeta^2} + U(\zeta) \right) \phi(\zeta) = \mathcal{M}^2 \phi(\zeta), \tag{23}$$

an effective single-variable light-front Schrödinger equation which is relativistic, covariant and analytically tractable. Using (16) one can readily generalize the equations to allow for the kinetic energy of massive quarks [5].

In the hard-wall model one has $U(z) = 0$; confinement is introduced by requiring the wavefunction to vanish at $z = z_0 \equiv 1/\Lambda_{\text{QCD}}$. In the case of the soft-wall model, the potential arises from a "dilaton" modification of the AdS metric; it has the form of a harmonic oscillator $U(z) = \kappa^4 z^2 + 2\kappa^2 (L + S - 1)$. The term $-(1 - 4L^2)/4z^2$ is a contribution to the LF kinetic energy induced by the change of variables to ζ.

Individual hadron states can be identified by their interpolating operator at $z \to 0$. For example, the pseudoscalar meson interpolating operator $\mathcal{O}_{2+L} = \bar{q}\gamma_5 D_{\{\ell_1} \cdots D_{\ell_m\}} q$, written in terms of the symmetrized product of covariant derivatives D with total internal space-time orbital momentum $L = \sum_{i=1}^m \ell_i$, is a twist-two, dimension $3 + L$ operator
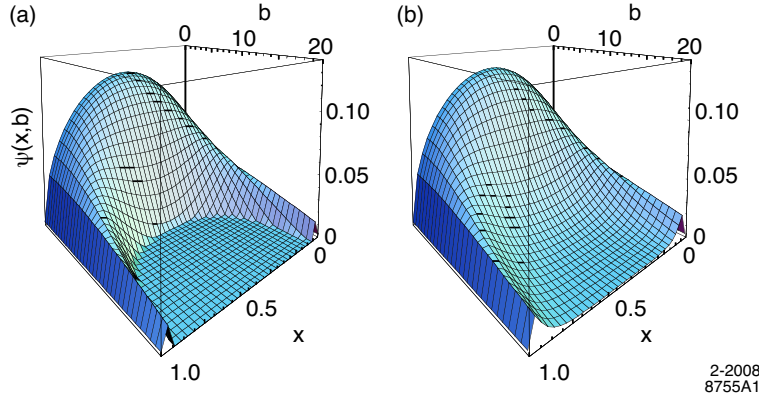
FIGURE 1. Pion light-front wavefunction $\psi_\pi(x, \mathbf{b}_\perp)$ for the AdS/QCD (a) hard=wall ($\Lambda_{QCD} = 0.32$ GeV) and (b) soft-wall ($\kappa = 0.375$ GeV) models.

with scaling behavior determined by its twist-dimension $2 + L$. Likewise the vector-meson operator $\mathscr{O}^\mu_{2+L} = \bar{q}\gamma^\mu D_{\{\ell_1} \cdots D_{\ell_m\}}q$ has scaling dimension $\Delta = 2 + L$. The scaling behavior of the scalar and vector AdS modes $\Phi(z) \sim z^\Delta$ at $z \to 0$ is precisely the scaling required to match the scaling dimension of the local pseudoscalar and vector-meson interpolating operators.

The resulting mass spectra for mesons at zero quark mass is $\mathscr{M}^2 = 4\kappa^2(n + L + S/2)$ in the soft-wall model. The spectral predictions for both light meson and baryon states are compared with experimental data in [5]. The corresponding wavefunctions (see fig. 1) display confinement at large interquark separation and conformal symmetry at short distances, reproducing dimensional counting rules for hard exclusive amplitudes.

VACUUM EFFECTS AND LIGHT-FRONT QUANTIZATION

The light-front vacuum is remarkably simple in light-cone quantization because of the restriction $k^+ \geq 0$. For example in QED, vacuum graphs such as $e^+e^-\gamma$ associated with the zero-point energy do not arise. In the Higgs theory, the usual Higgs vacuum expectation value is replaced with a $k^+ = 0$ zero mode [34]; however, the resulting phenomenology is identical to the standard analysis.

Hadronic condensates play an important role in quantum chromodynamics (QCD). Conventionally, these condensates are considered to be properties of the QCD vacuum and hence to be constant throughout spacetime. Recently we have presented [9, 35, 36] a new perspective on the nature of QCD condensates $\langle \bar{q}q \rangle$ and $\langle G_{\mu\nu}G^{\mu\nu} \rangle$, particularly where they have spatial and temporal support. Their spatial support is restricted to the interior of hadrons, since these condensates arise due to the interactions of quarks and gluons which are confined within hadrons. For example, consider a meson consisting of a light quark q bound to a heavy antiquark, such as a B meson. One can analyze the propagation of the light q in the background field of the heavy $\bar{b}$ quark. Solving the Dyson-Schwinger equation for the light quark one obtains a nonzero dynamical mass and, via the connection mentioned above, hence a nonzero value of the condensate $\langle \bar{q}q \rangle$.

But this is not a true vacuum expectation value; instead, it is the matrix element of the operator $\bar{q}q$ in the background field of the $\bar{b}$ quark. The change in the (dynamical) mass of the light quark in this bound state is somewhat reminiscent of the energy shift of an electron in the Lamb shift, in that both are consequences of the fermion being in a bound state rather than propagating freely. Similarly, it is important to use the equations of motion for confined quarks and gluon fields when analyzing current correlators in QCD, not free propagators, as has often been done in traditional analyses of operator products. Since after a $q\bar{q}$ pair is created, the distance between the quark and antiquark cannot get arbitrarily great, one cannot create a quark condensate which has uniform extent throughout the universe. The 55 orders of magnitude conflict of QCD with the observed value of the cosmological condensate is thus removed [36]. A new perspective on the nature of quark and gluon condensates in quantum chromodynamics is thus obtained: [9, 35, 36] the spatial support of QCD condensates is restricted to the interior of hadrons, since they arise due to the interactions of confined quarks and gluons. In the LF Theory, the condensate physics is replaced by the dynamics of higher non-valence Fock states. In particular, chiral symmetry is broken in a limited domain of size $1/m_\pi$, in analogy to the limited physical extent of superconductor phases. This picture explains the results of recent studies [37, 38, 39] which find no significant signal for the vacuum gluon condensate.

HADRONIZATION AT THE AMPLITUDE LEVEL

The conversion of quark and gluon partons is usually discussed in terms of on-shell hard-scattering cross sections convoluted with *ad hoc* probability distributions. The LF Hamiltonian formulation of quantum field theory provides a natural formalism to compute hadronization at the amplitude level [40]. In this case one uses light-front time-ordered perturbation theory for the QCD light-front Hamiltonian to generate the off-shell quark and gluon T-matrix helicity amplitude using the LF generalization of the Lippmann-Schwinger formalism:

$$T^{LF} = H_I^{LF} + H_I^{LF} \frac{1}{\mathcal{M}^2_{\text{Initial}} - \mathcal{M}^2_{\text{intermediate}} + i\varepsilon} H_I^{LF} + \cdots \qquad (24)$$

Here $\mathcal{M}^2_{\text{intermediate}} = \sum_{i=1}^{N} (\mathbf{k}^2_{\perp i} + m_i^2)/x_i$ is the invariant mass squared of the intermediate state and H_I^{LF} is the set of interactions of the QCD LF Hamiltonian in the ghost-free light-cone gauge [32]. The T^{LF}-matrix element is evaluated between the out and in eigenstates of H_{LF}^{QCD}. The event amplitude generator is illustrated for $e^+e^- \to \gamma^* \to X$ in Fig. 2.

The LFWFS of AdS/QCD can be used as the interpolating amplitudes between the off-shell quark and gluons and the bound-state hadrons. Specifically, if at any stage a set of color-singlet partons has light-front kinetic energy $\sum_i \mathbf{k}^2_{\perp i}/x_i < \Lambda^2_{\text{QCD}}$, then one coalesces the virtual partons into a hadron state using the AdS/QCD LFWFs. This provides a specific scheme for determining the factorization scale which matches perturbative and nonperturbative physics.

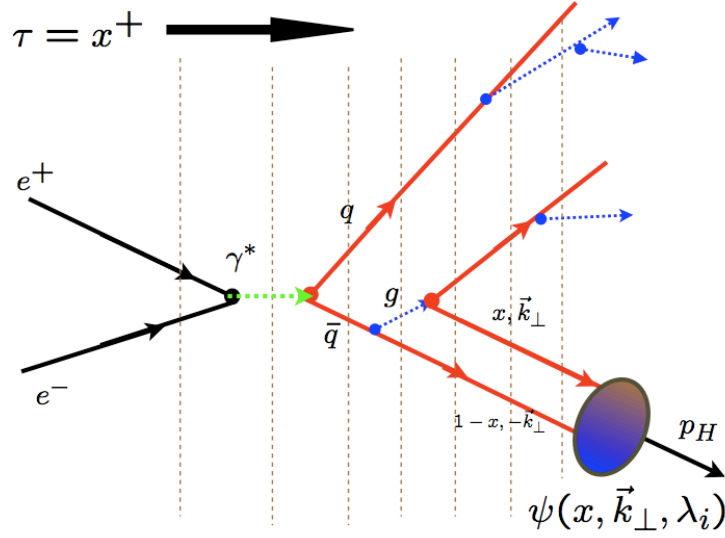This scheme has a number of important computational advantages:

FIGURE 2. Illustration of an event amplitude generator for $e^+ e^- \to \gamma^* \to X$ for hadronization processes at the amplitude level. Capture occurs if $\zeta^2 = x(1-x)\mathbf{b}_\perp^2 > 1/\Lambda_{QCD}^2$ in the AdS/QCD hard-wall model of confinement; i.e., if $\mathcal{M}^2 = \frac{\mathbf{k}_\perp^2}{x(1-x)} < \Lambda_{QCD}^2$.

(a) Since propagation in LF Hamiltonian theory only proceeds as τ increases, all particles propagate as forward-moving partons with $k_i^+ \geq 0$. There are thus relatively few contributing τ−ordered diagrams.

(b) The computer implementation can be highly efficient: an amplitude of order g^n for a given process only needs to be computed once. In fact, each non-interacting cluster within T^{LF} has a numerator which is process independent; only the LF denominators depend on the context of the process.

(c) Each amplitude can be renormalized using the "alternate denominator" counterterm method [41], rendering all amplitudes UV finite.

(d) The renormalization scale in a given renormalization scheme can be determined for each skeleton graph even if there are multiple physical scales.

(e) The T^{LF}-matrix computation allows for the effects of initial and final state interactions of the active and spectator partons. This allows for leading-twist phenomena such as diffractive DIS, the Sivers spin asymmetry and the breakdown of the PQCD Lam-Tung relation in Drell-Yan processes.

(f) ERBL and DGLAP evolution are naturally incorporated, including the quenching of DGLAP evolution at large x_i where the partons are far off-shell.

(g) Color confinement can be incorporated at every stage by limiting the maximum wavelength of the propagating quark and gluons.

(h) This method retains the quantum mechanical information in hadronic production amplitudes which underlie Bose-Einstein correlations and other aspects of the spin-statistics theorem. Thus Einstein-Podolsky-Rosen QM correlations are maintained even between far-separated hadrons and clusters.

A similar off-shell T-matrix approach was used to predict antihydrogen formation from virtual positron–antiproton states produced in $\bar{p}A$ collisions [42].

DYNAMICAL EFFECTS OF RESCATTERING

Initial- and final-state rescattering, neglected in the parton model, have a profound effect in QCD hard-scattering reactions, predicting single-spin asymmetries [43, 44], diffractive deep lepton-hadron inelastic scattering [45], the breakdown of the Lam Tung relation in Drell-Yan reactions [46], nor nuclear shadowing and non-universal antishadowing [47]—leading-twist physics which is not incorporated in the light-front wavefunctions of the target computed in isolation. It is thus important to distinguish [48] "static" or "stationary" structure functions which are computed directly from the LFWFs of the target from the "dynamic" empirical structure functions which take into account rescattering of the struck quark. Since they derive from the LF eigenfunctions of the target hadron, the static structure functions have a probabilistic interpretation. The wavefunction of a stable eigenstate is real; thus the static structure functions cannot describe diffractive deep inelastic scattering nor the single-spin asymmetries since such phenomena involves the complex phase structure of the $\gamma^* p$ amplitude. One can augment the light-front wavefunctions with a gauge link corresponding to an external field created by the virtual photon $q\bar{q}$ pair current [49, 50], but such a gauge link is process dependent [44], so the resulting augmented wavefunctions are not universal [45, 49, 51].

It should be emphasized that the shadowing of nuclear structure functions is due to the destructive interference between multi-nucleon amplitudes involving diffractive DIS and on-shell intermediate states with a complex phase. The physics of rescattering and shadowing is thus not included in the nuclear light-front wavefunctions, and a probabilistic interpretation of the nuclear DIS cross section is precluded. The distinction between static structure functions; i.e., the probability distributions computed from the square of the light-front wavefunctions, versus the nonuniversal dynamic structure functions measured in deep inelastic scattering is summarized in fig. 3.

CONCLUSIONS

Light-Front Holography is one of the most remarkable features of AdS/CFT. It allows one to project the functional dependence of the wavefunction $\Phi(z)$ computed in the AdS fifth dimension to the hadronic frame-independent light-front wavefunction $\psi(x_i, \mathbf{b}_{\perp i})$ in $3+1$ physical space-time. The variable z maps to $\zeta(x_i, \mathbf{b}_{\perp i})$. To prove this, we have shown that there exists a correspondence between the matrix elements of the electromagnetic current and the energy-momentum tensor of the fundamental hadronic constituents in QCD with the corresponding transition amplitudes describing the interaction of string modes in anti-de Sitter space with the external sources which propagate in the AdS interior. The agreement of the results for both electromagnetic and gravitational hadronic transition amplitudes provides an important consistency test and verification of holographic mapping from AdS to physical observables defined on the light-front. The transverse coordinate ζ is closely related to the invariant mass squared of the con-
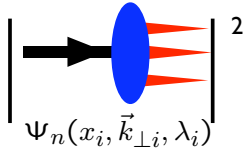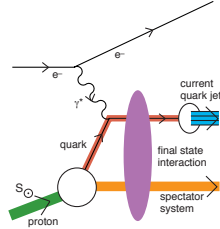
Static	**Dynamic**
• Square of Target LFWFs	Modified by Rescattering: ISI & FSI
• No Wilson Line	Contains Wilson Line, Phases
• Probability Distributions	No Probabilistic Interpretation
• Process-Independent	Process-Dependent - From Collision
• T-even Observables	T-Odd (Sivers, Boer-Mulders, etc.)
• No Shadowing, Anti-Shadowing	Shadowing, Anti-Shadowing, Saturation
• Sum Rules: Momentum and J^z	Sum Rules Not Proven
• DGLAP Evolution; mod. at large x	DGLAP Evolution
• No Diffractive DIS	Hard Pomeron and Odderon Diffractive DIS

FIGURE 3. Static versus dynamic structure functions

stituents in the LFWF and its off-shellness in the light-front kinetic energy, and it is thus the natural variable to characterize the hadronic wavefunction. In fact ζ is the only variable to appear in the light-front Schrödinger equations predicted from AdS/QCD.

The use of the invariant coordinate ζ in light-front QCD allows the separation of the dynamics of quark and gluon binding from the kinematics of constituent spin and internal orbital angular momentum. The result is a single-variable LF Schrödinger equation which determines the spectrum and LFWFs of hadrons for general spin and orbital angular momentum. This LF wave equation serves as a first approximation to QCD and is equivalent to the equations of motion which describe the propagation of spin-J modes on AdS [17]. This allows us to establish a gauge/gravity correspondence between an effective gravity theory on AdS$_5$ and light front QCD. The AdS/LF equations correspond to the kinetic energy terms of the partons inside a hadron, whereas the interaction terms build confinement. Since there are no interactions up to the confining scale in this approximation, there are no anomalous dimensions. The eigenvalues of these equations for both meson and baryons give a good representation of the observed hadronic spectrum, especially in the case of the soft-wall model. In the hard-wall model the orbital angular momentum decouples from the hadronic spin J and thus the LF excitation spectrum of hadrons depends only on orbital and principal quantum numbers. In the hard-wall model the dependence is linear: $\mathcal{M} \sim 2n + L$. In the soft-wall model the usual Regge behavior is found $\mathcal{M}^2 \sim n + L$. Both models predict the same multiplicity of states for mesons and baryons observed experimentally [52]. The predicted LFWFs have excellent phenomenological features, including predictions for the electromagnetic form factors

and decay constants. This may explain the experimental success of power-law scaling in hard exclusive reactions where there are no indications of the effects of anomalous dimensions.

Nonzero quark masses are naturally incorporated into the AdS/LF predictions [5] by including them explicitly in the LF kinetic energy $\sum_i (\mathbf{k}_{\perp i}^2 + m_i^2)/x_i$. Given the nonperturbative LFWFs one can predict many interesting phenomenological quantities such as heavy quark decays, generalized parton distributions and parton structure functions.

We also note the distinction between between static structure functions such as the probability distributions computed from the square of the light-front wavefunctions versus dynamical structure functions which include the effects of rescattering. We have also shown that the LF Hamiltonian formulation of quantum field theory provides a natural formalism to compute hadronization at the amplitude level.

The AdS/QCD model is semiclassical, and thus it only predicts the lowest valence Fock state structure of the hadron LFWF. One can systematically improve the holographic approximation by diagonalizing the QCD LF Hamiltonian on the AdS/QCD basis, or by generalizing the variational and other systematic methods used in chemistry and nuclear physics [53]. The action of the non-diagonal terms in the QCD interaction Hamiltonian also generates the form of the higher Fock state structure of hadronic LFWFs. In contrast with the original AdS/CFT correspondence, the large N_C limit is not required to connect light-front QCD to an effective dual gravity approximation.

ACKNOWLEDGMENTS

REFERENCES

1. J. M. Maldacena, Adv. Theor. Math. Phys. **2**, 231 (1998) [Int. J. Theor. Phys. **38**, 1113 (1999)] [arXiv:hep-th/9711200].
2. S. J. Brodsky and G. F. de Teramond, Phys. Rev. Lett. **96**, 201601 (2006) [arXiv:hep-ph/0602252].
3. S. J. Brodsky and G. F. de Teramond, Phys. Rev. D **77**, 056007 (2008) [arXiv:0707.3859 [hep-ph]].
4. S. J. Brodsky and G. F. de Teramond, Phys. Rev. D **78**, 025032 (2008) [arXiv:0804.0452 [hep-ph]].
5. S. J. Brodsky and G. F. de Teramond, arXiv:0802.0514 [hep-ph].
6. S. J. Brodsky and G. F. de Teramond, Phys. Lett. B **582**, 211 (2004) [arXiv:hep-th/0310227].
7. G. F. de Teramond and S. J. Brodsky, Phys. Rev. Lett. **94**, 201601 (2005).
8. A. Deur, V. Burkert, J. P. Chen and W. Korsch, Phys. Lett. B **665**, 349 (2008) [arXiv:0803.4119 [hep-ph]].
9. S. J. Brodsky and R. Shrock, Phys. Lett. B **666**, 95 (2008) [arXiv:0806.1535 [hep-th]].
10. J. M. Cornwall, Phys. Rev. D **26**, 1453 (1982).
11. G. Parisi, Phys. Lett. B **39**, 643 (1972).
12. S. J. Brodsky, Y. Frishman and G. P. Lepage, Phys. Lett. B **167**, 347 (1986).

13. J. Polchinski and M. J. Strassler, Phys. Rev. Lett. **88**, 031601 (2002) [arXiv:hep-th/0109174].
14. A. Karch, E. Katz, D. T. Son and M. A. Stephanov, Phys. Rev. D **74**, 015005 (2006) [arXiv:hep-ph/0602229].
15. J. Erlich, E. Katz, D. T. Son and M. A. Stephanov, Phys. Rev. Lett. **95**, 261602 (2005) [arXiv:hep-ph/0501128].
16. L. Da Rold and A. Pomarol, Nucl. Phys. B **721**, 79 (2005) [arXiv:hep-ph/0501218].
17. G. F. de Teramond and S. J. Brodsky, arXiv:0809.4899 [hep-ph].
18. S. J. Brodsky and G. R. Farrar, Phys. Rev. Lett. **31**, 1153 (1973).
19. V. A. Matveev, R. M. Muradian and A. N. Tavkhelidze, Lett. Nuovo Cim. **7** (1973) 719.
20. H. R. Grigoryan and A. V. Radyushkin, Phys. Rev. D **76**, 095007 (2007) [arXiv:0706.1543 [hep-ph]].
21. G. P. Lepage and S. J. Brodsky, Phys. Lett. B **87**, 359 (1979).
22. A. V. Efremov and A. V. Radyushkin, Phys. Lett. B **94**, 245 (1980).
23. E. M. Aitala *et al.* [E791 Collaboration], Phys. Rev. Lett. **86**, 4768 (2001) [arXiv:hep-ex/0010043].
24. H. M. Choi and C. R. Ji, Phys. Rev. D **74**, 093010 (2006) [arXiv:hep-ph/0608148].
25. P. A. M. Dirac, Rev. Mod. Phys. **21**, 392 (1949).
26. D. E. Soper, Phys. Rev. D **15**, 1141 (1977).
27. J. Polchinski and M. J. Strassler, JHEP **0305**, 012 (2003) [arXiv:hep-th/0209211].
28. X. D. Ji, Phys. Rev. Lett. **78**, 610 (1997) [arXiv:hep-ph/9603249].
29. O. V. Teryaev, arXiv:hep-ph/9904376.
30. S. J. Brodsky, D. S. Hwang, B. Q. Ma and I. Schmidt, Nucl. Phys. B **593**, 311 (2001) [arXiv:hep-th/0003082].
31. Z. Abidin and C. E. Carlson, Phys. Rev. D **77**, 095007 (2008) [arXiv:0801.3839 [hep-ph]].
32. S. J. Brodsky, H. C. Pauli and S. S. Pinsky, Phys. Rept. **301**, 299 (1998) [arXiv:hep-ph/9705477].
33. G. P. Lepage and S. J. Brodsky, Phys. Rev. D **22**, 2157 (1980).
34. P. P. Srivastava and S. J. Brodsky, Phys. Rev. D **66**, 045019 (2002) [arXiv:hep-ph/0202141].
35. S. J. Brodsky and R. Shrock, arXiv:0803.2541 [hep-th].
36. S. J. Brodsky and R. Shrock, arXiv:0803.2554 [hep-th].
37. B. L. Ioffe and K. N. Zyablyuk, Eur. Phys. J. C **27**, 229 (2003) [arXiv:hep-ph/0207183].
38. M. Davier, A. Hocker and Z. Zhang, Nucl. Phys. Proc. Suppl. **169**, 22 (2007) [arXiv:hep-ph/0701170].
39. M. Davier, S. Descotes-Genon, A. Hocker, B. Malaescu and Z. Zhang, Eur. Phys. J. C **56**, 305 (2008) [arXiv:0803.0979 [hep-ph]].
40. S. J. Brodsky, G. de Teramond and R. Shrock, AIP Conf. Proc. **1056**, 3 (2008) [arXiv:0807.2484 [hep-ph]].
41. S. J. Brodsky, R. Roskies and R. Suaya, Phys. Rev. D **8**, 4574 (1973).
42. C. T. Munger, S. J. Brodsky and I. Schmidt, Phys. Rev. D **49**, 3228 (1994).
43. S. J. Brodsky, D. S. Hwang and I. Schmidt, Phys. Lett. B **530**, 99 (2002) [arXiv:hep-ph/0201296].
44. J. C. Collins, Phys. Lett. B **536**, 43 (2002) [arXiv:hep-ph/0204004].
45. S. J. Brodsky, P. Hoyer, N. Marchal, S. Peigne and F. Sannino, Phys. Rev. D **65**, 114025 (2002) [arXiv:hep-ph/0104291].
46. D. Boer, S. J. Brodsky and D. S. Hwang, Phys. Rev. D **67**, 054003 (2003) [arXiv:hep-ph/0211110].
47. S. J. Brodsky, I. Schmidt and J. J. Yang, Phys. Rev. D **70**, 116003 (2004) [arXiv:hep-ph/0409279].
48. S. J. Brodsky, arXiv:0811.0875 [hep-ph].
49. A. V. Belitsky, X. Ji and F. Yuan, Nucl. Phys. B **656**, 165 (2003) [arXiv:hep-ph/0208038].
50. J. C. Collins and A. Metz, Phys. Rev. Lett. **93**, 252001 (2004) [arXiv:hep-ph/0408249].
51. J. C. Collins, Acta Phys. Polon. B **34**, 3103 (2003) [arXiv:hep-ph/0304122].
52. E. Klempt and A. Zaitsev, Phys. Rept. **454**, 1 (2007) [arXiv:0708.4016 [hep-ph]].
53. J. P. Vary, H. Honkanen, Jun Li, P. Maris, S. J. Brodsky, P. Sternberg, E G. Ng, C. Yang arXiv:0812.1819 [nucl-th].